

FINITE ELEMENT GALERKIN MODELS AND IDENTIFIED FINITE ELEMENT MODELS - A COMPARATIVE STUDY.

Stephen A. Billings, Daniel Coca

*Department of Automatic Control & Systems Engineering, University of
Sheffield, Mappin Street, Sheffield, S1 3JD, UK*

Abstract:

A new approach to derive a finite element discretisation of PDE equations solely from observations is compared, in terms of approximation accuracy, with the standard finite element Galerkin approach which assumes knowledge of the governing PDE's. It is shown both in theory and by means of an example that, for a given model order, the identified model is more accurate than the equivalent finite element Galerkin approximation derived from the original PDE's.

Keywords: Distributed-Parameter Systems, Finite Element Solutions, Identification Algorithms, Interpolation Approximation, System Identification.

1. INTRODUCTION

The numerical computation of the solution of PDE's and of the control laws associated with a distributed parameter system is often based on a finite dimensional discretisation of the original PDE. A well known approach is the finite element Galerkin method (Brenner and Ridgway Scott, 1994).

The standard method of discretisation however assumes a complete knowledge of the governing PDE's for the system of interest. But in many cases the evolution equations will not be known a priori and only measurements of the state (solution) of the system are available. In a companion paper (Coca and Billings, 2002), a new approach to derive a finite element discretisation of PDE equations from experimental measurements using system identification has been introduced to address this kind of problem.

The identification data could represent a video recording of patterns in a chemical reaction or the paper profile measured using a full-web measurement system in a paper making process, for example. In another scenario, the data could be the result of a high order numerical simulation of a known PDE. The proposed identification approach can be used to derive a simpler, reduced order model which preserves accuracy and

which is much less expensive from a computational point of view.

The proposed approach involves two basic steps, the finite element approximation of the variables in the spatial domain and the identification of the finite dimensional model from the time-dependent coordinate vector respectively.

Transforming the original, infinite dimensional system of PDE's into a finite dimensional problem poses at least two very important questions. The first is whether or not the finite dimensional discretisation of say, order n , converges to the true solution as $n \rightarrow \infty$. The second question is how to choose the right order of approximation knowing that if the order is too small the finite element solution will provide a poor approximation to the original PDE solution or even display qualitatively different behaviour. On the other hand, choosing a very fine finite element approximation subspace, that is a large n , will result in large scale finite dimensional models which are not always convenient for real-time control applications involving dynamic optimisation because this would lead to a significant increase in the computational work.

The convergence of the identified finite dimensional models has been established in (Coca and Billings, 2002) for a class of linear first order systems. With regard to the issue of model order, the proposed approach allows optimisation of the number of degrees of freedom by projecting the initial interpolation onto a suitable coarser finite element subspace subject to predefined accuracy constraints.

In the standard finite element Galerkin method, reducing the order of approximation by using a coarser approximation subspace ignores the 'high frequency' components of the solution lying in the orthogonal subspace with negative effects on the behaviour and accuracy of the approximate solution.

The aim of this paper is to analyse the effects of the reduction in the model order on the approximation accuracy of the identified finite element models derived from spatio-temporal measurements. Theoretically, it is shown that the identified models are more accurate than the models derived by the standard finite element approach with respect to the same finite element basis. The analysis is supplemented by test computations which confirm the theoretical results.

2. THE EVOLUTION EQUATION

Let H be a separable real Hilbert space with inner product $\langle \cdot, \cdot \rangle$ and norm $|\cdot|$ and V another separable Hilbert space which is embedded continuously and densely in H . Here H is identified with its own dual space. Let V^* denote the dual space of V and $\|\cdot\|_*$ denote the norm on V^* . It follows that $V \subset H \subset V^*$ with continuous and dense embeddings. The following inequality is assumed to hold

$$|\varphi| \leq \lambda^{-1/2} \|\varphi\| \quad (1)$$

Consider the following evolution equation

$$\frac{du}{dt} + Au = v(t) \quad (2)$$

$$u(0) = u_0 \in H \quad (3)$$

with A a bounded linear, coercive operator ($\langle A\varphi, \varphi \rangle \geq \alpha \|\varphi\|^2$, $\varphi \in V$ for some $\alpha > 0$), $v(t, x) \in C(\mathbb{R}_+; H) \cap L^2(0, T; H)$, $T > 0$, bounded in $C(\mathbb{R}_+; H)$. The initial value problem (2), (3) has a unique solution $u(t, x)$ defined for all $t > 0$ such that $u \in C(\mathbb{R}_+; H) \cap L^2(0, T; V)$, $\forall T > 0$.

The equation (2) is usually complemented by boundary conditions which can be of the Dirichlet, Neumann or periodicity type for example. These can be accommodated by considering restrictions of A and v to corresponding closed subspaces V

3. THE IDENTIFICATION METHOD

The identification method proposed in (Coca and Billings, 2002) can be viewed as an *inverse* finite element Galerkin approach where the solution is used to derive the finite dimensional model rather than the original PDE's.

To account for the fact that in general it is not possible to measure the full state (solution) of the system, an observation operator $\mathcal{Z} : C([0, T], C(\Omega)) \rightarrow \mathcal{Y}$ is introduced as follows

$$y_{N,n} = \mathcal{Z}u = \{u(t_i, x_j)\}_{i=1, \dots, N}^{j=1, \dots, n} \quad (4)$$

where $\mathcal{Y} = \mathbb{R}^{N \times n}$ is the *observation space* to which the measurements $y = \mathcal{Z}u$ belong. This requires that both $u(t, x)$ and $v(t, x)$ are continuous with respect to x .

It is assumed that point measurements are recorded from a finite number of locations distributed uniformly over the spatial domain with a sampling step Δx (i.e. the data is spatially sampled at the $n - 1$ nodal points $\frac{1}{n}, \frac{2}{n}, \dots, \frac{n-1}{n}$) and that the data is also sampled uniformly over the time interval $[0, T]$ with a sampling time Δt . In practice it is assumed that both $\Delta x = \frac{1}{n}$ and Δt are sufficiently small so that the full behaviour of the solution u is captured.

Let V^n be a finite dimensional subspace of V . The identification problem is to determine, based only on the given set of discrete observations $y_{N,n} = \{u(t_i, x_j)\}_{i=1, \dots, N}^{j=1, \dots, n}$ and $v_{N,n} = \{v(t_i, x_j)\}_{i=1, \dots, N}^{j=1, \dots, n}$ a finite dimensional dynamical system whose solution u_n approximates the observed dynamical behaviour in V^n .

The identification is performed in two stages. In the first stage the data is interpolated onto a finite element subspace V^n . This involves computing the input and output coordinate vectors relative to the finite element basis. The second stage involves estimating a finite dimensional, discrete-time model which approximates this input/output behaviour.

A common choice of finite element subspaces V^n on Ω are the spaces of continuous piecewise polynomial functions defined with respect to a uniform mesh on Ω . For simplicity it is assumed that $\Omega = (0, 1)$.

Let $\{\varphi_j^n\}_{j=0}^n$ be the standard l th order B-spline base (de Boor, 1978). In this case $V^n = \text{span}\{\varphi_j^n\}_{j=0}^n$ and V is the Sobolev space $H^1(0, 1)$.

Note that $\bigcup_{n=0}^{\infty} V^n$ is dense in $H = L^2(0, 1)$ and $H^1(0, 1)$.

Let

$$y_n(t, x) = \sum_{j=0}^n y_{n,j}(t) \varphi_j^n(x), \quad t > 0 \quad (5)$$

$$v_n(t, x) = \sum_{j=0}^n v_{n,j}(t) \varphi_j^n(x) \quad t > 0 \quad (6)$$

denote the interpolation of u and v respectively in V^n .

It was shown in (Coca and Billings, 2002) that the input/output behaviour $\mathbf{v}_n(t) = (v_{n,0}(t), \dots, v_{n,n}(t))$, $\mathbf{y}_n(t) = (y_{n,0}(t), \dots, y_{n,n}(t))$ can be approximated by the following differential equation

$$\frac{du_n}{dt} + A_n u_n = v_n(t), \quad (7)$$

$$u_n(0) = y_n(0) \quad (8)$$

where $A_n : V^n \rightarrow V^n$ is a finite dimensional operator defined by

$$\langle A_n u_n, \varphi^n \rangle = \langle A_n u_n, \varphi^n \rangle, \quad \varphi^n \in V^n \quad (9)$$

for any $u_n \in V^n \subset H$.

More precisely it was shown that the solution $u_n(t, x)$ to (7) remains in a bounded set of $L^\infty(\mathbb{R}_+; H)$ and that $u_n(t, x) \rightarrow y_n(t, x)$ strongly in $L^2(0, T, H)$ and in $L^2(0, T, V)$ as $n \rightarrow \infty$.

Assuming that V^n is a high order approximation subspace, let V^m be the coarser subspace such that $V^m \subset V^n$ and let

$$\begin{aligned} y_m &= P_m y_n = \sum_{j=0}^m y_{m,j}(t) \varphi_j^m(x) \\ u_m &= P_m u_n = \sum_{j=0}^m y_{m,j}(t) \varphi_j^m(x) \\ v_m &= P_m v_n = \sum_{j=0}^m v_{m,j}(t) \varphi_j^m(x) \end{aligned} \quad (10)$$

be the orthogonal projections of y_n (the approximation of u in V^n), u_n and v_n respectively on the coarser subspace V^m and

$$\begin{aligned} u_{n-m} &= Q_{n-m} u_n = \sum_{j=1}^{n-m} u_{n-m,j}(t) \psi_j^{n-m}(x) \\ v_{n-m} &= Q_{n-m} v_n = \sum_{j=1}^{n-m} v_{n-m,j}(t) \psi_j^{n-m}(x) \end{aligned} \quad (11)$$

be the projection of u_n and v_n respectively on the orthogonal subspace W^{n-m} of V^m in V^n spanned by the basis $\{\psi_j^{n-m}\}_{j=1}^{n-m}$.

Corollary 3.1. With the notation introduced above it follows that:

- a) $u_m(t, x) \rightarrow y_m(t, x)$ strongly in $L^2(0, T; H)$ and $L^2(0, T; V)$ as $n \rightarrow \infty$.
- b) $\mathbf{u}_m(t) \rightarrow \mathbf{y}_m(t)$ in $L^2(0, T, l^2(0, \infty))$ as $n \rightarrow \infty$.

Proof: Projecting equation (7) on V^m and W^{n-m} respectively leads to the following dynamical system

$$\frac{du_m}{dt} + P_m A_n (u_m + u_{n-m}) = v_m(t), \quad (12)$$

$$\frac{du_{n-m}}{dt} + Q_{n-m} (A_n u_m + u_{n-m}) = v_{n-m}(t)$$

with initial conditions, $u_m(0) = P_m y_n(0)$ and $u_{n-m}(0) = Q_{n-m} y_n(0)$.

The convergence results a) and b) follow as a consequence of Theorem 3.1 in (Coca and Billings, 2002).

Remark 3.1. Assuming that only u_m is observable and that the system (12) admits an external differential representation (input/output equation) with inputs \mathbf{v}_m , \mathbf{v}_{n-m} and output \mathbf{u}_m it follows that based on the inputs \mathbf{v}_m , \mathbf{v}_{n-m} and the outputs \mathbf{y}_m it should be possible to estimate an input/output dynamical representation to approximate the dynamics in the coarser space V^m which according to Corollary 3.1 converges to the interpolate y_m and to the true solution u as $n \rightarrow \infty$.

The resulting model provides a better description for the dynamics in the V^m subspace than a standard Galerkin approximation, involving the same number of equations, because the input/output model derived from (12) accounts for the dynamics of the small scale structures in the complementary subspace W^{n-m} represented by the coupling term $P_m A_n u_{n-m}$ in (12)).

In numerical simulation, an initial high dimensional approximation on a fine grid, could be replaced with a discrete-time approximation of lower dimension obtained from data generated by the high-dimensional model using a system identification approach. The resulting discrete-time model will be able to predict better the low-frequency part of the PDE solutions than the standard Galerkin approximation involving the same number of equations.

Assuming that the data used in identification is the result of numerical simulation, let $y_n = u_n$ and u^m be the solutions of the Galerkin approximation of order n and m respectively, with $n > m$. Recalling the minimum distance properties of the projection $u_m = P_m u_n$ with respect to u_n , let $e_m = u_m - u^m$ be the approximation error, relative to u_m , of the low-order Galerkin approximation in V^m .

It easy to show that e_m satisfies the following error equation

$$\left\langle \frac{de_m}{dt}, \varphi^m \right\rangle + \langle A e_m, \varphi^m \rangle + \langle u_{n-m}, \varphi^m \rangle = 0 \quad (13)$$

for any $\varphi^m \in V^m$. By taking $\varphi^m = e_m$ and thanks to the coercivity of A it follows that

$$\frac{1}{2} \frac{d}{dt} |e_m|^2 + \alpha \|e_m\|^2 \leq |e_m| |u_{n-m}| \quad (14)$$

and subsequently after using twice (1) that

$$\frac{d}{dt} |e_m|^2 + \alpha \lambda |e_m|^2 \leq \frac{1}{\alpha \lambda} |u_{n-m}| \quad (15)$$

Integrating (15) and using the classical Gronwall lemma yields

$$|e_m|^2 \leq |e_m(0)|^2 e^{-\alpha\lambda t} + \frac{|u_{n-m}|_s^2}{(\alpha\lambda)^2} (1 - e^{-\alpha\lambda t}) \quad (16)$$

where $|u_{n-m}|_s^2 = \sup_{t \in [0, \infty)} \{|u_{n-m}(t)|^2\}$, which provides an upper bound for $e_m(t)$ in $L^\infty(\mathbb{R}_+; H)$.

4. NUMERICAL EXAMPLE

This section provides a comparison of the quantitative approximation properties of the identified finite element model and the model derived by using the standard finite element Galerkin approach for the following diffusion equation

$$\frac{\partial u(t, x)}{\partial t} - c \frac{\partial^2 u(t, x)}{\partial x^2} = 0, \quad (17)$$

with domain $\Omega = (0, 1)$, initial conditions

$$u(0, x) = \begin{cases} 2Bx & x \in (0, 0.5) \\ 2B - 2Bx & x \in (0.5, 1) \end{cases} \quad (18)$$

and Dirichlet boundary conditions. In this case $H = L^2(0, 1)$ and V is the Sobolev space $H_0^1(0, 1)$ endowed with the usual inner products and corresponding induced norms.

The operator $A \in \mathcal{L}(V, V^*)$ is given by

$$\langle A, \varphi, \psi \rangle = \int_0^1 D\varphi(x) D\psi(x) dx \quad (19)$$

with $\varphi, \psi \in H_0^1(0, 1)$. It is easy to see that assumptions (A1) and (A2) are verified in this case.

For $B = \pi^2$ the exact solution $u(t, x)$ of the initial value problem (17), (18) is given by the following series expansion

$$u(t, x) = \sum_{k=1}^{\infty} \frac{8(-1)^{k-1}}{(2k-1)^2} e^{-c(2k-1)^2 \pi^2 t} \cdot \sin((2k-1)\pi x). \quad (20)$$

The solution, based on the first 50 terms of the expansion (20) with $c = 1.0$ was sampled uniformly in both the spatial and time domain with $\Delta x = 1/128$ and $\Delta t = 0.5 \times 10^{-3}$.

From each location $N=1000$ data points were generated. The data were interpolated using linear B-spline functions. The initial interpolated solution involving 127 basis functions was subsequently projected onto a lower approximation subspace and expressed in terms of only 15 basis functions.

One thousand samples shown in figure 1, corresponding to the output vector $\mathbf{y}_n(t) = (y_{n,1}(t), \dots, y_{n,15}(t))$, were used for identification. The data were used to estimate a deterministic MIMO-AR model (not given here

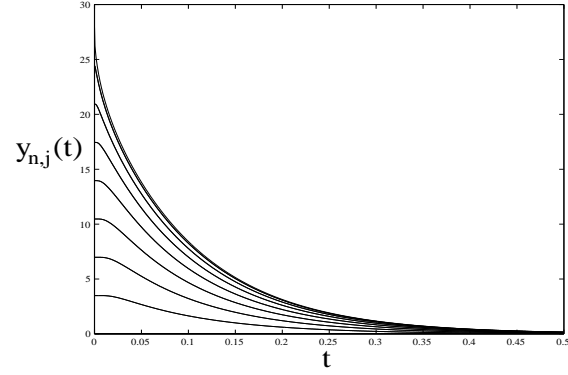


Fig. 1. Coordinate vector $\mathbf{y}_n(t)$

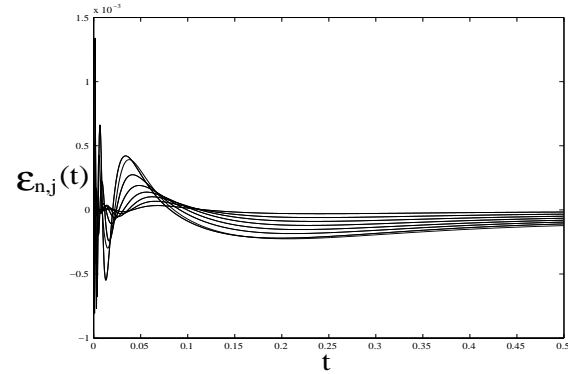


Fig. 2. Prediction error $\hat{\mathbf{y}}_n(t) - \mathbf{u}^n(t)$ for the identified MIMO-AR model.

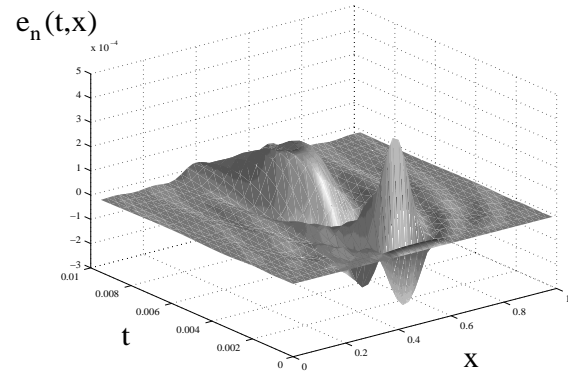


Fig. 3. Approximation error $e_n(t, x) = \hat{y}_n(t, x) - u^n(t, x)$ of the solution in V^n ($n = 16$).

for reasons of space). The selection of the linear terms included in each of the 15 subsystems was performed with the help of the Orthogonal Forward Regression algorithm (Billings *et al.*, 1988).

The model was simulated and the resulting model predicted output was compared with the coordinate vector $\mathbf{u}^n(t)$ corresponding to the orthogonal projection of the original solution $u^n = P_n u(t, x)$ on the approximation subspace V^n $\mathbf{y}_n(t)$. The prediction error vector $\boldsymbol{\varepsilon}_n(t) = \hat{\mathbf{y}}_n(t) - \mathbf{u}^n(t)$ is plotted in figure 2 and the corresponding approximation error of the solution in the V^n subspace $e_n(t, x) = \hat{y}_n(t, x) - u^n(t, x)$ is plotted in figure 3.

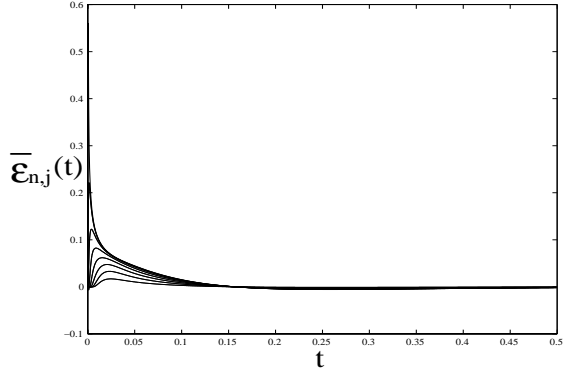


Fig. 4. Prediction error $\bar{\mathbf{u}}_n(t) - \mathbf{u}^n(t)$ for the standard Galerkin model.

A standard finite element Galerkin discretisation was derived using the same linear B-splines basis with $n = 16$, defined with respect to the uniform mesh $0, \frac{1}{n}, \frac{2}{n}, \dots, 1$. This leads to the following system of differential equations

$$M^n \frac{d}{dt} \bar{\mathbf{u}}^n(t) = K^n \bar{\mathbf{u}}^n(t) \quad (21)$$

where M^n denotes the Gramm matrix corresponding to the linear B-spline basis $\{\varphi_j^n\}_{j=1}^5$

$$M^n = [M_{i,j}^n] = \left[\int_0^1 \varphi_i^n(x) \varphi_j^n(x) dx \right] \quad (22)$$

and the stiffness matrix K is given by

$$K^n = [K_{i,j}^n] = \left[\int_0^1 D\varphi_i^n(x) D\varphi_j^n(x) dx \right] \quad (23)$$

The system was integrated using a stiff differential equation solver with a very fine integration step $dt = 0.25 \cdot 10^{-4}$. The resulting coordinate vector $\bar{\mathbf{u}}^n(t)$ was compared with the same coordinate vector $\mathbf{u}^n(t)$ corresponding to the orthogonal projection of the original solution on the approximation subspace V^n . The error vector $\bar{\epsilon}_n(t) = \bar{\mathbf{u}}^n(t) - \mathbf{u}^n(t)$ is shown in figure 2 and the corresponding approximation error $e^n(t, x) = \bar{\mathbf{u}}^n(t, x) - \mathbf{u}^n(t, x)$ in V^n is shown in figure 3.

From the figures 2, 3, 4 and 5 it is evident that the identified model approximates far better the solution of the original PDE equation in the V^n subspace than the finite element Galerkin discretisations derived over the same finite dimensional approximation subspace. In particular the NRMSE of $\epsilon_n(t)$ is $0.3 \cdot 10^{-2} \%$ compared with the NRMSE of $\bar{\epsilon}_n(t)$ which is 0.58 %.

In order to compare the two models in terms of number of parameters, equation (21) is written in equivalent form as

$$\frac{d}{dt} \bar{\mathbf{u}}^n(t) = (M^n)^{-1} K^n \bar{\mathbf{u}}^n(t) \quad (24)$$

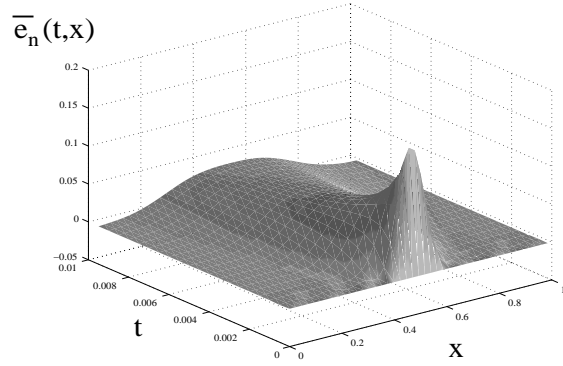


Fig. 5. Approximation error $e_n(t, x) = \hat{y}_n(t, x) - u^n(t, x)$ of the solution in V^n ($n = 16$).

which has 225 nonzero parameters compared with the estimated discrete-time MIMO-AR model which has only 97 parameters.

Moreover, it should be noted that the model (21) is a continuous-time model which should have been further discretised in time in order to perform a fair comparison. The process of translating (21) into a discrete-time model, will normally introduce additional approximation errors or could produce an unstable model.

5. CONCLUSIONS

The above analysis has shown that the finite element discretisation obtained by system identification are more accurate and more parsimonious than the standard finite element Galerkin discretisations derived over the same finite dimensional approximation subspace.

The system identification approach analysed in this paper can be used both when the governing evolution equations which characterise a distributed parameter system are known and in the cases when only process measurements are available. When the PDE's are known an initial high-order approximation derived by standard discretisation methods from the known equations can be replaced by a simpler model estimated from the simulated data.

6. ACKNOWLEDGEMENTS

The authors fully acknowledge that this work was supported by the Engineering and Physical Sciences Research Council, UK.

7. REFERENCES

- Billings, S. A., S. Chen and M. J. Kronenberg (1988). Identification of MIMO non-linear systems using a forward-regression orthogonal estimator. *Int. J. Control* **49**, 2157–2189.

- Brenner, S. C. and L. Ridgway Scott (1994). *The Mathematical Theory of Finite Element Methods*. Vol. 1. Springer Verlag.
- Coca, D. and S. A. Billings (2002). Identification of finite-dimensional models for distributed-parameter systems. *15th IFAC World Congress on Automatic Control, July 21-26, Barcelona, Spain*.
- de Boor, C. (1978). *A practical guide to splines*. Springer Verlag.